

Epitaxial growth of conductive LaNiO_3 thin films by pulsed laser ablation

Tao Yu ^{a,*}, Yan-Feng Chen ^a, Zhi-Guo Liu ^a, Xiao-Yuan Chen ^a,
Li Sun ^a, Nai-Ben Ming ^a, Lian-Jie Shi ^b

^a National Laboratory of Solid State Microstructures, Nanjing University and Center for Advanced Studies in Science and Technology of Microstructures, Nanjing 210093, China

^b Department of Material Science and Technology, Nanjing University of Science and Technology, Nanjing 210014, China

Received 31 July 1995; accepted 4 August 1995

Abstract

Epitaxial LaNiO_3 (LNO) thin films have been fabricated on (001) SrTiO_3 and (001) LaAlO_3 single crystal substrates by pulsed laser ablation at 30 Pa oxygen partial pressure and 700°C substrate temperature. X-ray θ - 2θ scan, X-ray Φ scan, Rutherford backscattering (RBS) channeling and electron probe technique were used to characterize the as-deposited LNO thin films. The surface of the epitaxial LNO thin film was analyzed by X-ray photoelectron spectroscopy (XPS). Down to 80 K, the epitaxial LNO thin film showed good metallic behavior and its resistivity was $2.5 \times 10^{-6} \Omega \text{ m}$ at 300 K.

Keywords: Lanthanum nickel oxide; LaNiO_3 ; Perovskite; Thin film laser ablation; Metallic; Ohmic contacts; SrTiO_3 ; LaAlO_3 substrates

The ternary compound LaNiO_3 (LNO) has a perovskite structure with pseudocubic lattice parameter $a = 3.84 \text{ \AA}$. It has been reported that LNO without any doping is a Pauli paramagnetic material and an n-type metallic oxide (the resistivity at 300 K is near $10^{-5} \Omega \text{ m}$) [1,2]. Because LNO has the desirable metallic conducting properties, it can be used as an ohmic contact electrode material.

In the last few years, ferroelectric thin films have attracted much attention, primarily because of their potential applications as nonvolatile ferroelectric random access memories (FRAM). [3] In these applications, it is essential to fabricate high quality ferroelectric thin films on proper electrode materials. In recent studies, the metallic oxides, such as $\text{YBa}_2\text{Cu}_3\text{O}_{7-x}$ (YBCO), $\text{La}_{0.5}\text{Sr}_{0.5}\text{CoO}_3$ (LSCO),

RuO_2 , and IrO_2 , have been used as electrodes in ferroelectric capacitors [4–6]. Because the structure of LNO is compatible with the ferroelectric materials such as PbTiO_3 (PT), $\text{PbZr}_x\text{Ti}_{1-x}\text{O}_3$ (PZT) and $\text{Pb}_x\text{La}_{1-x}\text{Zr}_y\text{Ti}_{1-y}\text{O}_3$ (PLZT), it is a favorable candidate as the electrode for epitaxial growth of ferroelectric thin films. In order to fabricate epitaxial ferroelectric thin films on LNO, the preparation of epitaxial LNO films is important. Epitaxial LNO films have been successfully grown as a lattice matched metallic buffer layer for YBCO [7]. The work for growing $\text{Bi}_2\text{VO}_{5.5}$ thin films with LNO electrodes has been reported by Prasad et al. [8]. In this paper we report on preparation of epitaxial conductive LNO thin films on (001) SrTiO_3 (STO) and (001) LaAlO_3 (LAO) single crystal substrates by pulsed laser ablation (PLA). X-ray θ - 2θ scan, X-ray Φ scan, Ruther-

* Corresponding author.

ford backscattering (RBS) channeling, electron probe technique and X-ray photoelectron spectroscopy (XPS) were used to characterize the structure and chemical composition of epitaxial LNO thin films. Down to 80 K, the epitaxial LNO thin film showed good metallic conductive properties and its resistivity was $2.25 \times 10^{-6} \Omega \text{ m}$ at 300 K.

In our experiment, the PLA processes were performed by using a Lambda Physik LPX205i KrF excimer laser system with the 248 nm radiation in wavelength, 30 ns in pulse width and 5 Hz in pulse frequency. The laser beam was focused onto a rotating polycrystalline LNO target with a size of $\phi 20 \times 2 \text{ mm}^3$, which was prepared by the solid state reaction of La_2O_3 and Ni_2O_3 (the molar ratio was 1 : 1). The average laser pulse energy density was 200 mJ/mm^2 . The plume of ejected material from the target was collected onto a substrate mounted on a resistively heated stage whose temperature varied from 25 to 800°C . The target and substrate stage were set inside the deposition chamber with a background vacuum of $2 \times 10^{-5} \text{ Pa}$. The substrates used in our experiment were (001) SrTiO_3 (STO) and (001) LaAlO_3 (LAO) single crystals. Typical oxygen partial pressure and substrate temperature were 30 Pa and 700°C respectively during laser ablation. The deposition time was 30 min. After deposition the films were kept at 700°C in 0.2 atm oxygen for 30 min and then cooled to room temperature at a rate of 10°C/min . The thickness of the films was about 300 nm.

As-deposited LNO films on STO and LAO exhibited a dense, shiny and dark appearance. Fig. 1 is a scanning electron micrograph of the surface of LNO/STO, which shows that the LNO film grown by PLA has very good quality, the film surface is very smooth and there is not any droplet on it.

The chemical composition of LNO thin films was analyzed by a JAX-8800M electron probe microanalyzer. The acceleration voltage was 15 kV in electron probe analysis. The result showed that the La : Ni ratio was 0.51 : 0.49. This indicated that the composition of the LNO thin film was stoichiometric.

The structure of LNO films was characterized by X-ray θ - 2θ scan using Cu $K\alpha$ radiation on a Rigaku diffractometer. Fig. 2 is the X-ray θ - 2θ scan pattern of the LNO film on the STO substrate (Fig. 2a) and on the LAO substrate (Fig. 2b). In Figs. 2a and 2b only the (001) and (002) diffraction peaks of the LNO film

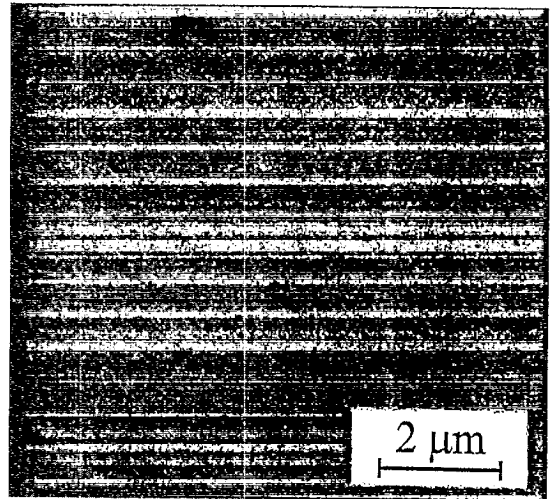


Fig. 1. Scanning electron micrograph of the surface of the LNO thin film grown on STO.

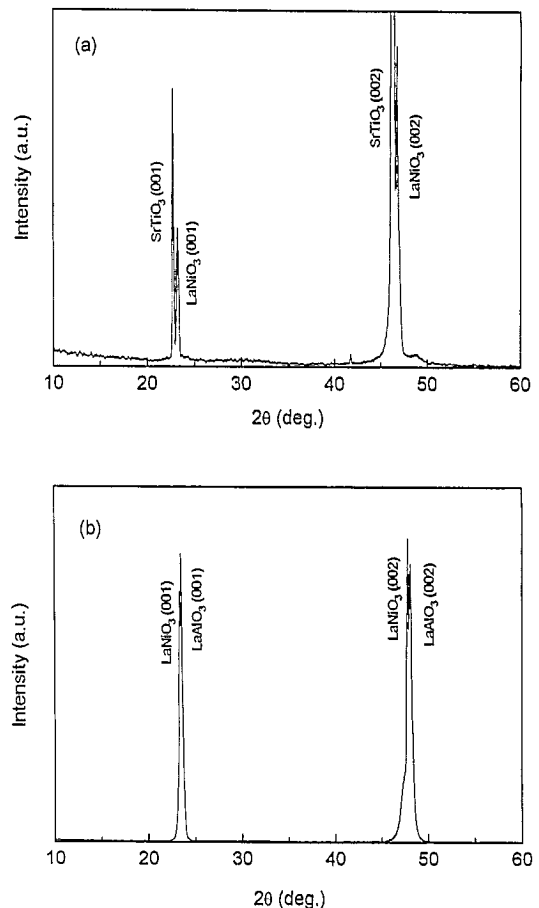


Fig. 2. The X-ray θ - 2θ scan pattern of the LNO film grown on (a) (001)STO and (b) grown on (001)LAO.

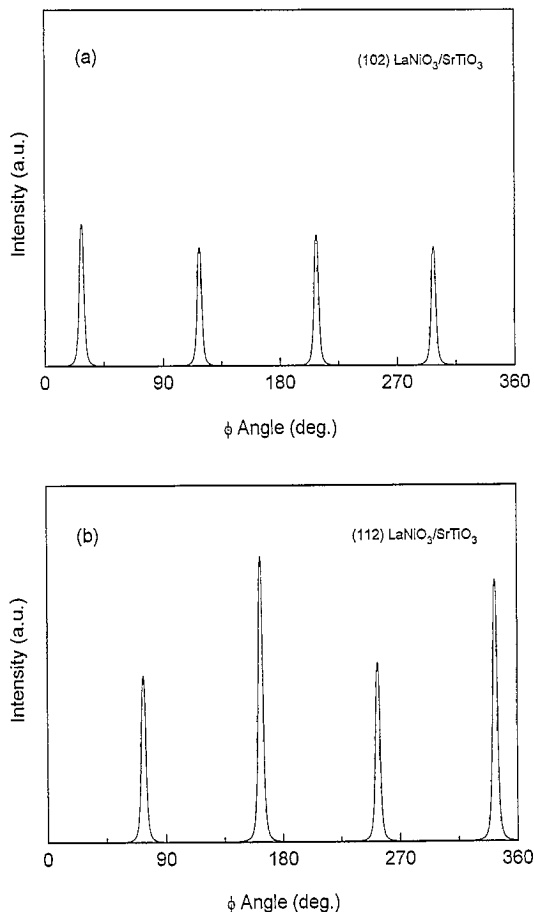


Fig. 3. The X-ray Φ scan of (a) (102)LNO/STO and (b) (112)LNO/STO.

can be recognized. This indicates that the LNO film is either highly $\langle 001 \rangle$ oriented or grown epitaxially on STO and LAO substrates.

X-ray Φ scan and RBS channeling technique were carried out to confirm the epitaxial growth of LNO thin films. In X-ray Φ scan measurements of LNO/STO, (102) and (112) planes of the LNO film were selected. When Ψ , the tilt angle of the surface normal of the LNO film, was 26.57° and 2θ was fixed at 53.15° , the (102)LNO/STO Φ scan result was obtained by rotating the sample 0° – 360° around the surface normal. This result is plotted in Fig. 3a. Fig. 3b is the Φ scan result of (112)LNO/STO when Ψ was 35.26° and 2θ was 58.69° in the experiment. In Fig. 3a or 3b, four equally spaced peaks separated by 90° were observed. The peak in Fig. 3b was shifted by 45° with respect to that in Fig. 3a. This agreed with the theoretical angle between (102) and (112) planes of LNO in X-ray Φ scan meas-

urements. In addition, the X-ray Φ scans of the (102) and (112) planes of the STO substrate were measured at the same time and the peaks were aligned with the (102) and (112) planes of the LNO thin film respectively. So, Fig. 3 clearly indicates that the LNO film was epitaxially grown on the STO substrate [7]. The epitaxial growth of LNO on the LAO substrate was also confirmed by X-ray Φ scans.

The RBS channeling study was carried out on LNO/LAO. Fig. 4 shows the 2 MeV He^+ ion Rutherford random backscattering and channeling spectra of an as-deposited LNO film on the LAO substrate. In the random backscattering spectrum, the peaks of La, Ni and O in the thin film can be recognized. The peak of La became wide because of the contribution of the La element in the LAO substrate. In Fig. 4, the minimum yield $\chi_{\min} = 18\%$ indicates that the LNO thin film on the LAO substrate was of very good crystallinity.

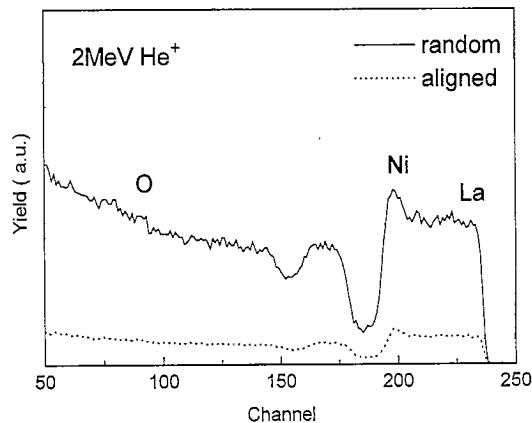


Fig. 4. Random and channeling Rutherford backscattering patterns of LNO/LAO.

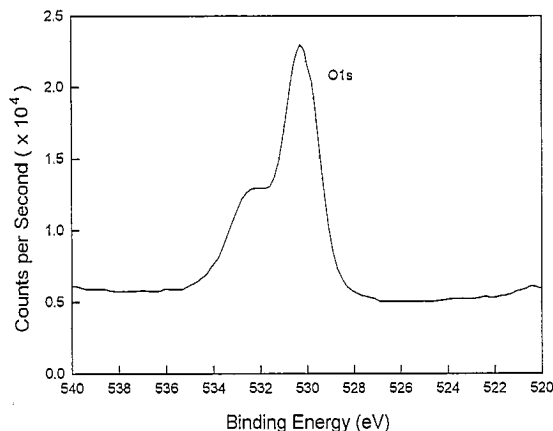


Fig. 5. The O1s region of XPS of the epitaxial LNO thin film.

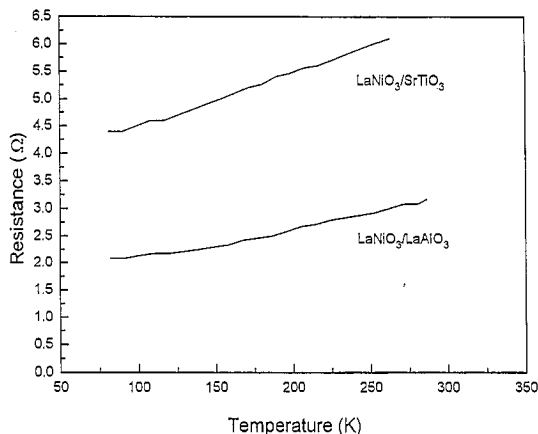


Fig. 6. Resistance versus temperature curves of epitaxial LNO thin films.

The surface of the epitaxial LNO thin film was analyzed by X-ray photoelectron spectroscopy (XPS) employing a VGS-5000 electron spectrometer. Fig. 5 is the O1s region of XPS of the epitaxial LNO thin film. In Fig. 5, two peaks can be found. The peak of lower binding energy corresponds to the lattice oxygen in LNO. Another peak of higher binding energy may arise from surface disorder or O^- ions on the surface of the LNO thin film [9]. Because the depth of XPS analysis is limited (< 2 nm), the XPS result gave the surface information of the epitaxial LNO thin film. Fig. 5 indicates that there were oxygen vacancy or chemical adsorptional oxygen on the surface of the epitaxial LNO thin film. These oxygen vacancy or chemical adsorptional oxygen may have influence on the fabrication and ferroelectric properties of ferroelectric thin films deposited on epitaxial LNO thin film electrodes.

The resistance versus temperature of LNO/STO and LNO/LAO were measured by the standard dc four-point probe method below 300 K. The result is plotted in Fig. 6. The resistance versus temperature plots are reasonably linear in this figure. Down to 80 K, the LNO thin films showed good metallic behavior and the resistivity was $2.25 \times 10^{-6} \Omega \text{ m}$ at 300 K.

In conclusion, epitaxial LNO thin films have been fabricated on STO and LAO single crystal substrates by the PLA method. The electron probe analysis showed the stoichiometric growth of LNO thin films. The epitaxial LNO thin films were characterized by X-ray $\theta-2\theta$ scan, X-ray Φ scan and RBS channeling study. XPS analysis showed that there were oxygen vacancy and chemical adsorptional oxygen on the surface of the epitaxial LNO thin film. The metallic conductive properties of LNO thin films were measured by the four-point probe method.

Acknowledgements

The authors would like to thank Professor Yong-Shu Jin and Professor Cheng-Yi Lin for the help in experiments. The project was supported by the 863 National High Technology Program and the National Natural Science Foundation of P.R. China.

References

- [1] A. Wold, B. Post and E. Banks, *J. Am. Chem. Soc.* 70 (1957) 4911.
- [2] K.P. Rajeev, G.V. Shivakumar and A.K. Raychaudhuri, *Solid State Commun.* 79 (1991) 591.
- [3] J.F. Scott and C.A. Paz de Araujo, *Science* 246 (1989) 1400.
- [4] R. Ramesh, W.K. Chan, B. Wilkens, H. Gilchrist, T. Sands, J.M. Tarascon, V.G. Keramidias, D.K. Fork, J.J. Lee and A. Safari, *Appl. Phys. Letters* 61 (1992) 1537.
- [5] J.T. Cheung, P.E.D. Morgan and R. Neurgaonkar, *Proc. 4th. Intern. Symp. Integrated Ferroelectric (Colorado Springs, 1992)* p. 518.
- [6] T. Nakamura, Y. Nakao, A. Kamisawa and H. Takasu, *Japan. J. Appl. Phys.* 33 (1994) 5207.
- [7] K.M. Satyalakshmi, R.M. Mallya, K.V. Ramanathan, X.D. Wu, B. Brainard, D.C. Gautier, N.Y. Vasanthacharya and M.S. Hegde, *Appl. Phys. Letters* 62 (1993) 1233.
- [8] K.V.R. Prasad, K.B.R. Varma, A.R. Raju, K.M. Satyalakshmi, R.M. Mallya and M.S. Hegde, *Appl. Phys. Letters* 63 (1993) 1898.
- [9] J.P. Kemp and P.A. Cox, *Solid State Commun.* 75 (1990) 731.